



How to Calculate Adsorption Isotherms of Particles Using Two-Parameter Monolayer Adsorption Models and Equations

*Risti Ragadhita, Asep Bayu Dani Nandiyanto**

Departemen Kimia, Universitas Pendidikan Indonesia

Correspondence: E-mail: nandiyanto@upi.edu

ABSTRACT

Adsorption isotherm is the most important calculation to predict and analyze the various possible mechanisms that occur in adsorption process. However, until now, most studies only presented the adsorption isotherm theory, and there are no studies that explain the adsorption isotherm thoroughly and in detail from theory to calculation. Therefore, this study contains guidelines for selecting the type of adsorption isotherm to describe the entire adsorption data set, which is featured by the ten most common adsorption isotherms. The steps of how to analyze the two-parameter monolayer adsorption are presented. This study is expected to provide clear and useful information for researchers who are working and studying on the adsorption process.

© 2021 Tim Pengembang Jurnal UPI

ARTICLE INFO

Article History:

Submitted/Received 15 Nov 2020

First revised 30 Des 2020

Accepted 24 Feb 2021

First available online 28 Feb 2021

Publication date 01 Apr 2021

Keyword:

*Adsorption Isotherms,
Carbon,
Curcumin,
Education,
Silica,
Tungsten.*

1. INTRODUCTION

Adsorption is a surface phenomenon that involves adhesion of atoms, ions or molecules from a gas, liquid, or dissolved solid on a surface of substance. The atoms, ions or molecules that attached on the solid surface is the adsorbate, and the place where the adsorbate accumulates is called the adsorbent. This process creates a film of the adsorbate on the surface of the adsorbent. Definition of adsorption is different from absorption. The absorption involves a fluid (as the absorbate) is dissolved by or permeates a liquid or solid (the absorbent), and the process involves the whole volume of the material. Illustration from the definition of adsorbate and adsorbent is presented in **Figure 1**.

Adsorption divided into two types based on molecular interactions: physical and chemical adsorptions (Al-Ghouti & Da'ana, 2020; Kong & Adidharma, 2019). Adsorption process is widely applied and well-practiced in water treatment, purification, and separation processes. This process is also one of the most effective and promising techniques, supported by facile, technically feasible, and economical processes (Rahmani & Sasani, 2016; Hegazi, 2013).

One of the important factors in the adsorption is adsorption isotherm. The

relationship in the adsorption isotherm explains the phenomena and interactions between adsorbate and adsorbent. Generally, the adsorption performance can be predicted by modeling the adsorption isotherm data because the adsorption isotherm model can provide information about the adsorbent capacity, the adsorption mechanism, and the evaluation of the adsorption process performance (Nandiyanto *et al.*, 2020a; Anshar & Raya, 2016). In previous studies, we have performed isotherm analysis on various adsorbent systems (Nandiyanto *et al.*, 2020a; Nandiyanto *et al.*, 2020b; Nandiyanto *et al.*, 2020c; Nandiyanto *et al.*, 2020d). In this study, we used the most widely applied isotherm models to evaluate adsorption performance, such as Langmuir, Freundlich, Temkin, Dubinin-Radushkevich, Florry-Huggins, Fowler-Guggenheim, Hill-Deboer, Jovanovic, Harkin-Jura, and Halsey, while other researches only described the theory and the calculation method was not discussed deeply. This study was also completed with the calculation strategies for getting the parameters in the adsorption isotherm.

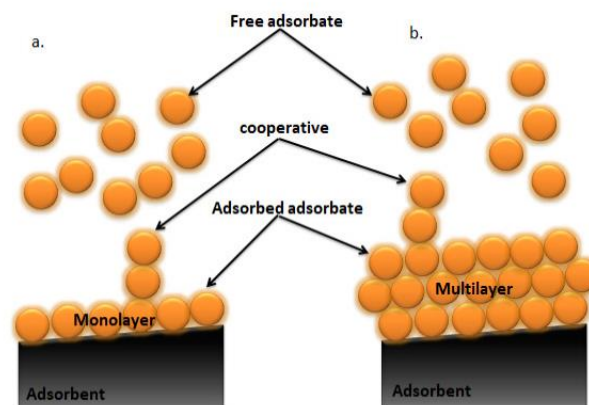


Figure 1. Illustration of monolayer (a) and multilayer (b) adsorption process (Rina Maryanti *et al.*, 2020)

2. ADSORPTION ISOTHERM THEORY

2.1. Langmuir Isotherm

Langmuir isotherm defines that the maximum adsorbent capacity occurs due to the presence of a single layer (monolayer) of adsorbate on the adsorbent surface. There are four assumptions in this type of isotherm, namely (Langmuir, 1918):

- The molecules are adsorbed by a fixed site (the reaction site at the adsorbent surface).
- Each site can "hold" one adsorbate molecule.
- All sites have the same energy.
- There is no interaction between the adsorbed molecules and the surrounding sites. Adsorption process form monolayer. Illustration of monolayer formation during adsorption is shown in **Figure 1 (a)**.

Langmuir isotherm model is represented by **equation (1)**:

$$\frac{1}{Q_e} = \frac{1}{Q_{max}K_L} \frac{1}{C_e} + \frac{1}{Q_{max}} \quad (1)$$

where Q_e is the amount of adsorbed adsorbate molecule per gram of adsorbent (mg/g), Q_{max} is the capacity of the adsorbent monolayer (mg/g), C_e is the adsorbate equilibrium concentration (mg/L), and K_L is the Langmuir adsorption constant.

The important factor in the Langmuir isotherm is the dimensionless constant or separation factor (R_L) (Langmuir, 1918) which is expressed by **equation (2)**:

$$R_L = \frac{1}{1+K_L C_e} \quad (2)$$

This separation factor has the following values:

- $R_L > 1$, unfavorable adsorption process (allows the adsorption process to occur, most desorption processes occur).
- $R_L = 1$, linear adsorption process (depending on the amount adsorbed and the concentration adsorbed).
- $R_L = 0$, Irreversible adsorption process (strong adsorption).

$0 < R_L < 1$, Favorable adsorption process (normal adsorption).

2.2. Freundlich Isotherm

Freundlich isotherm describes a physical type of adsorption in which the adsorption occurs in several layers and the bonds are not strong (multilayer). Multilayer formation is illustrated in **Figure 1 (b)**. Freundlich isotherm also assumes that the sites of adsorption are heterogeneous (Dada *et al.*, 2012). The empirical relationship for expressing Freundlich isotherm is given in **equation (3)**:

$$\ln Q_e = \ln K_f + \frac{1}{n} \ln C_e \quad (3)$$

where K_f is Freundlich constant, C_e is the concentration of adsorbate under equilibrium conditions (mg/L), Q_e is the amount of adsorbate absorbed per unit of adsorbent (mg/g), and n is the value indicating the degree of linearity between the adsorbate solution and the adsorption process (Dada *et al.*, 2012). The value of n is described as follows:

- $n = 1$, linear adsorption.
- $n < 1$, adsorption process with chemical interaction.
- $n > 1$, adsorption process with physical interaction.
- Favorable adsorption process is declared when $0 < 1/n < 1$, and a cooperative adsorption process occurs when $1/n > 1$.

2.3. Temkin Isotherm

Temkin isotherm assumes three postulates, namely that the adsorption heat decreases linearly with increasing surface adsorbent coverage, the adsorption process assumes a uniform binding energy distribution on the adsorbent surface, and the adsorption interaction involves the interaction between adsorbate-adsorbent (Romero-Gonzales *et al.*, 2005). Temkin isotherm is given in **equation (4)**:

$$Q_e = B_T \ln A_T + B_T \ln C_e \quad (4)$$

where B_T is the adsorption heat constant (if the $B_T < 8$ kJ/mol, the adsorption process occurs physically), A_T is the binding equilibrium constant, and T is the absolute temperature.

2.4. Dubinin-Radushkevich Isotherm

Dubinin-Radushkevich isotherm expresses the adsorption process on the adsorbent which has a pore structure or adsorbent which has a heterogeneous surface and expresses the adsorption free energy. its adsorption process is based on micropore volume filling (Romero-Gonzales *et al.*, 2005). Dubinin-Radushkevich isotherm is written in **equation (5)**:

$$\ln Q_e = \ln Q_s - (\beta \varepsilon^2) \quad (5)$$

where β is the Dubinin-Radushkevich isotherm constant, Q_s refers to the saturation capacity of theoretical isotherms, and ε is the Polanyi potential (J/mol) is calculated using **equation (6)**:

$$\varepsilon = RT \ln \left[1 + \frac{1}{C_e} \right] \quad (6)$$

To calculate the free energy of adsorption per adsorbate molecule, it is calculated using **equation (7)**:

$$E = \frac{1}{\sqrt{2\beta}} \quad (7)$$

where C_e is the equilibrium concentration of solute and E is the adsorbate energy per molecule as the energy needed to remove molecules from the surface. The equation describes:

- (i) $E < 8$ kJ/mol, physical adsorption.
- (ii) $8 < E < 168$ kJ/mol, chemical adsorption.

2.5. Jovanovic Isotherm

Jovanovic isotherm is based on the assumptions found in the Langmuir model, without allows some mechanical contact between the adsorbate and the adsorbent (Ayawei *et al.*, 2017). The linear correlation of

the Jovanovic model is shown in **equation (8)**:

$$\ln Q_e = \ln Q_{max} - K_J C_e \quad (8)$$

where Q_e is the amount of adsorbate in the adsorbent at equilibrium (mg/g), Q_{max} is the maximum uptake of adsorbate, and K_J is the Jovanovic constant.

2.6. Halsey Isotherm

Halsey isotherm evaluates a multilayer adsorption system (Dada *et al.*, 2012). The Halsey model follows **equation (9)**:

$$Q_e = \frac{1}{n_H} \ln K_H - \left(\frac{1}{n_H} \right) \ln C_e \quad (9)$$

where K_H dan n are the Halsey model constants.

2.7. Harkin-Jura Isotherm

Harkin-Jura isotherm describes that the adsorption occurring on the adsorbent surface is a multilayer adsorption because the adsorbent has a heterogeneous pore distribution (Ayawei *et al.*, 2017). This model is expressed by **equation (10)**:

$$\frac{1}{q_e^2} = \frac{\beta_{HJ}}{A_{HJ}} - \left(\frac{1}{A} \right) \log C_e \quad (10)$$

where β_{HJ} value is related to specific surface area of adsorbent and A_{HJ} are the Harkin Jura isotherm constants.

The modification of the Harkin-Jura equation (**equation 10**) is used to determine the surface area of the adsorbent. The modified Harkin-Jura equation is written in **equation (11)**.

$$\beta_{HJ} = \frac{-q(S^2)}{4.606RTN} \quad (11)$$

Where q is the constant independent of the nature of the adsorbent, S is the specific surface area ($\frac{m^2}{g}$), R is the universal gas constant ($8.314 \frac{J}{mol \cdot K}$), T is the absolute temperature, and N is the Avogadro number.

Then, the specific surface area of adsorbent is determined by **equation (12)**.

$$S^2 = -\frac{\beta_{HJ} \times 4.606RTN}{q} \quad (12)$$

For surface area calculations, **Table 1** shows several of q value.

Table 1. List of q_{value} various material. Recalculated from reference ([Shanavas et al., 2011](#); [Nandiyanto et al., 2020g](#))

Material	T (K)	$q\left(\frac{m^2}{g}\right)$
Carbon	298	1.053×10^{21}
	308	$1,760 \times 10^{21}$
	313	1.727×10^{21}
	318	1.677×10^{21}
	323	1.662×10^{21}
	328	1.664×10^{21}
Titanium Dioxide	308	1.011×10^{24}
	313	6.631×10^{23}
	318	4.552×10^{23}
	323	4.553×10^{23}
	328	2.633×10^{23}
Silica	298	3.436×10^{22}
Tungsten Trioxide (WO ₃)	298	1.141×10^{24}

2.8. Flory-Huggins Isotherm

Flory-Huggins isotherm takes into account the degree of surface coverage of the adsorbate on the adsorbent. This isotherm also assumes that the adsorption process occurs spontaneously ([Saadi et al., 2015](#)). Flory-Huggins isotherm is expressed by **equation (13)**:

$$\log \frac{\theta}{C_e} = \log K_{FH} + n \log(1 - \theta) \quad (13)$$

where $\theta = \left(1 - \frac{C_e}{C_o}\right)$ is the degree of surface coverage, K_{FH} is the Flory–Huggins model equilibrium constant and n_{FH} is the number of adsorbates occupying adsorption site. Furthermore, the Gibbs free energy of spontaneity (ΔG^0) is calculated from the equilibrium constant (K_{FH}). The value of ΔG^0 corresponds to the K_{FH} value as shown in **equation (14)**:

$$\Delta G^0 = -RT \ln K_{FH} \quad (14)$$

The negative sign on the value ΔG^0 confirms that the adsorption process is spontaneous, which is a function of temperature (T).

2.9. Fowler-Guggenheim Isotherm

Fowler-Guggenheim isotherm suggests that there is a lateral interaction at a set of localized sites with weak interactions (Van der Waals interaction effect) between adsorbed species at neighboring sites ([Hamdaoui and Naffrechoux, 2007](#)). The empirical relationship of Fowler-Guggenheim model is expressed by **equation (15)**:

$$\ln \left(\frac{C_e(1-\theta)}{\theta} \right) - \frac{\theta}{1-\theta} = -\ln K_{FG} + \frac{2W\theta}{RT} \quad (15)$$

where K_{FG} is the constant, W (kJ/mol) for the adsorbed adsorbate at the active site representing the interaction between the adsorbate and the adsorbent, C_e is the equilibrium constant, W is the empirical interaction energy between two adsorbed molecules at the adjacent neighboring site (kJ/mol), and θ is the fractional coverage of the surface. The empirical interaction energy (W) has the following value:

- (i) If $W > 0$ kJ/mol, attractive interaction between adsorbed molecule.
- (ii) If $W < 0$ kJ/mol, repulsive interaction between adsorbed molecule.
- (iii) If $W = 0$ kJ/mol, no interaction between adsorbed molecule.

2.10. Hill-Deboer Isotherm

Hill-Deboer isotherm describes mobile adsorption and bilateral interactions between adsorbed molecules (Hamdaoui and Naffrechoux, 2007). Hill-Deboer isotherm approach is written in **equation (16)**:

$$\ln \left[\frac{C_e(1-\theta)}{\theta} \right] - \frac{\theta}{1-\theta} = -\ln K_1 - \frac{K_2 \theta}{RT} \quad (16)$$

where K_1 is the Hill-Deboer constant (L/mg) and K_2 is the energetic constant of the interactions between adsorbed molecules (kJ/mol):

- (i) $K_2 > 0$ kJ/mol, attraction between adsorbed molecules.
- (ii) $K_2 < 0$ kJ/mol, repulsion between adsorbed molecules.
- (iii) $K_2 = 0$ kJ/mol, no interaction between adsorbed molecules.

The quantity adsorbed by the unit mass of the adsorbent at equilibrium (Q_e) is calculated using **equation (17)**:

$$Q_e = \frac{C_0 - C_e}{m} \times V \quad (17)$$

where C_0 is the initial concentration (mg/L), C_e is the concentration at equilibrium (mg/L), m is the mass of the adsorbent (grams), and V is the volume of the adsorbate solution (L).

3. MATERIAL AND METHOD

There were several materials used as adsorbents which were the result of conversion from agricultural waste such as carbon converted from peanut shells (CPS), carbon obtained from rice husks (CRH), silica from rice husks (SRH). Inorganic materials such as tungsten (WO_3) was also used as adsorbents in this study. Detailed information on how the process of converting agricultural waste into carbon and silica and fabrication process of WO_3 was presented in our previous studies (Ragadhita *et al.*, 2019; Faardini *et al.*, 2020; Nandiyanto *et al.*, 2020a; Nandiyanto *et al.*, 2017;

Nandiyanto *et al.*, 2020e). The adsorbate solution used as an experimental model was curcumin solution. Information on curcumin production was carried out in the same manner as provided in our previous study (Ragadhita *et al.*, 2019; Nandiyanto *et al.*, 2020f).

In general, the adsorption process was carried out in the following steps: specific mass amount of each CPS, CRH, SRH, and WO_3 adsorbents were put into 200 mL of curcumin solution with variations concentrations of 20, 40, 60, 80 ppm at constant pH and temperature. The solution mixture was mixed in a borosilicate batch (glass reactor) with a capacity of 400 mL and has dimensions of 10 and 8 cm, respectively, for height and diameter.

Then, the solution mixture was stirred at 1000 rpm for 1 h. Next, the solution mixture was filtered. The filtrate was measured and analyzed with a UV-VIS spectrophotometer (Model 7205; JENWAY; Cole-Parmer; US; analyzed at wavelengths between 200 and 600 nm).

After the adsorption process was completed, the next step was to evaluate the adsorption process. Several adsorption isotherm models were used for the analysis of the adsorption process including Langmuir, Freundlich, Temkin, Dubinin-Radushkevich, Florry-Huggins, Fowler-Guggenheim, Hill-Deboer, Jovanovic, Halsey, and Harkin-Jura isotherms.

4. RESULTS AND DISCUSSION

4.1. Linearization and Curve Plotting to Obtain Two-Parameter Adsorption Isotherms from Several Models

The adsorption process includes a series of adsorption experiments to calculate the adsorption parameters used to express the adsorption equilibrium model. Several adsorption isotherm models were used to evaluate the adsorption process in this study are Langmuir, Freundlich, Temkin, Dubinin - Raduschkevich, Flory-Huggins, Fowler-

Guggenheim, Hill-Deboer, Jovanovic, Harkin-Jura, and Halsey isotherms. The calculation of the adsorption isotherm is carried out through data fitting to obtain a linear equation ($y = mx + c$). Then, we also need to consider the value of R^2 . The greater R^2 relates to similarity data to the model proposed. The fitting of this data is adjusted to the linear expression of the mathematical model of each adsorption isotherm. From the results of the data fitting, several parameters in the adsorption process were obtained. The phenomena occurring during the adsorption were predicted. Information regarding curve data fitting, calculations, and parameters of the adsorption isotherm model that must be analyzed is presented in **Table 2**.

4.2. Experimental Results from The Adsorption Process

Data from the adsorption process of curcumin solution using CPS, CRH, SRH, and WO_3 adsorbents are presented in **Table 3**. **Table 3** shows the adsorption data of curcumin solution for data fitting using two-parameter isotherm adsorptions: Langmuir, Freundlich, Temkin, Dubinin-Radushkevich, Jovanovic, Halsey, Harkin-Jura, Flory-Huggins, Fowler-Guggenheim, and Hill-Deboer isotherm.

4.3. Plotting Analysis for Adsorption Isotherms using a Two-Parameter Adsorption Isotherm

4.3.1 Langmuir

Langmuir model adsorption parameters were obtained using **equation (1)** as

presented as $\frac{1}{Q_e} = \frac{1}{Q_{max}K_L} \frac{1}{C_e} + \frac{1}{Q_{max}}$. To get the Langmuir model parameters, we need to convert C_e and Q_e values into the form of $\frac{1}{C_e}$ and $\frac{1}{Q_e}$, which are used for fitting data (see **Table 2**).

The curves of fitting data result from **equation (1)** are presented in **Figures 2 (a-d)**. The result of fitting data was used to determine the adsorption parameters. The result of data fitting in the form of a gradient obtained is the $\frac{1}{Q_{max} \times K_L}$ value and the intercept is the $\frac{1}{Q_{max}}$ value. **Table 4** show parameters of the Langmuir model using CPS, CRH, SRH, and WO_3 adsorbents.

Q_{max} and K_L in **Table 4** are the maximum monolayer adsorption capacity and Langmuir adsorption constant, respectively. Based on Q_{max} value, adsorption process using CRH adsorbent is very good due to it has the highest maximum monolayer adsorption capacity (Q_{max}) value than others. Langmuir adsorption constant (K_L) shows the degree adsorbate-adsorbent interaction. Higher K_L value indicating strong adsorbate-adsorbent interaction while smaller K_L value indicating weak interaction between adsorbate molecule and adsorbent surface. The K_L value for all adsorption systems show a relatively small value means weak interaction between the adsorbent and adsorbate molecules due to the active site only adsorb one molecule. Plotting analysis shows that CPS, SRH, and WO_3 have relatively high correlation value ($R^2 > 0.70$) than CRH, informing that CPS, SRH, and WO_3 are good represented by Langmuir isotherm.

Table 2. Information regarding curve data fitting, calculation, and isotherm parameters

Isotherm Type	Linier Equation	Plotting	Parameter
Langmuir	$\frac{1}{Q_e} = \frac{1}{Q_{max}K_L C_e} + \frac{1}{Q_{max}}$	$1/C_e$ vs $1/Q_e$	<ul style="list-style-type: none"> $\frac{1}{Q_{max}} = \text{intercept}$ $Q_{max} = \frac{1}{\text{intercept}}$ $K_L = \frac{1}{Q_{max} \times \text{slope}}$
Freundlich	$\ln Q_e = \ln k_f + \frac{1}{n} \ln C_e$	$\ln C_e$ vs $\ln Q_e$	<ul style="list-style-type: none"> $\ln K_F = \text{intercept}$ $K_F = e^{\text{slope}}$ $\frac{1}{n_F} = \text{slope}$ $n_F = \frac{1}{\text{slope}}$
Temkin	$q_e = B_T \ln A_T + B_T \ln C_e$	$\ln C_e$ vs Q_e	<ul style="list-style-type: none"> $B = \text{slope}$ $\ln A_T = \frac{\text{intercept}}{B_T}$ $B_T = \frac{RT}{B}$
Dubinin-Radushkevich	$\ln q_e = \ln q_s - (\beta \epsilon^2)$	ϵ^2 vs $\ln Q_e$	<ul style="list-style-type: none"> $\beta = K_{DR} = \text{slope}$ $E = \frac{1}{\sqrt{2 \times K_{DR}}}$
Flory Huggins	$\log \frac{\theta}{C_e} = \log K_{FH} + n \log(1 - \theta)$	$\log \left(\frac{\theta}{C_0} \right)$ vs $\log(1 - \theta)$	<ul style="list-style-type: none"> $n_{FH} = \text{slope}$ $\log k_{FH} = \text{intercept}$ $K_{FH} = 10^{\text{intercept}}$ $\Delta G^\circ = RT \ln(k_{FH})$ $\theta = 1 - \left(\frac{C_e}{C_0} \right)$
Fowler-Guggenheim	$\ln \left(\frac{C_e(1 - \theta)}{\theta} \right) - \frac{\theta}{1 - \theta} = -\ln K_{FG} + \frac{2W\theta}{RT}$	$\frac{\theta}{\ln \left[\frac{C_e(1 - \theta)}{\theta} \right]}$ vs $\frac{\theta}{1 - \theta}$	<ul style="list-style-type: none"> $W = \text{slope}$ $-\ln K_{FG} = \text{intercept}$ $K_{FG} = e^{-\text{intercept}}$ $\alpha (\text{slope}) = \frac{2W\theta}{RT}$ $W = \frac{RT\alpha}{2\theta}$ $\theta = 1 - \left(\frac{C_e}{C_0} \right)$
Hill-Deboer	$\ln \left[\frac{C_e(1 - \theta)}{\theta} \right] - \frac{\theta}{1 - \theta} = -\ln K_1 - \frac{K_2\theta}{RT}$	$\frac{\theta}{\ln \left[\frac{C_e(1 - \theta)}{\theta} \right]}$ vs $-\frac{\theta}{1 - \theta}$	<ul style="list-style-type: none"> $-\ln k_1 = \text{intercept}$ $\alpha (\text{slope}) = \frac{k_2\theta}{RT}$ $k_2 = \frac{RT\alpha}{\theta}$ $\theta = 1 - \left(\frac{C_e}{C_0} \right)$
Jovanovic	$\ln q_e = \ln q_{max} - K_j C_e$	C_e vs $\ln Q_e$	<ul style="list-style-type: none"> $K_j = \text{slope}$ $\ln Q_{max} = \text{intercept}$ $Q_{max} = e^{\text{intercept}}$
Harkin-Jura	$\frac{1}{q_e^2} = \frac{B}{A} - \left(\frac{1}{A} \right) \log C_e$	$\log C_e$ vs $\frac{1}{q_e^2}$	<ul style="list-style-type: none"> $A_H = \frac{1}{\text{slope}}$ $\frac{B_H}{A_H} = \text{intercept}$
Halsey	$\ln Q_e = \frac{1}{n_H} \ln K_H - \frac{1}{n_H} \ln C_e$	$\ln C_e$ vs $\ln Q_e$	<ul style="list-style-type: none"> $\frac{1}{n_H} = \text{slope}$ $\frac{1}{\text{slope}} = n_H$ $\ln K_H = \text{intercept}$ $K_H = e^{\text{intercept}}$

Table 3. Curcumin solution adsorption data using CPS, CRH, SRH, and WO₃ adsorbents

Adsorbent	C _i (ppm)	C _e (ppm)	q _e (mg/L)	ε ²	θ
CPS	15	15	1.45	14.43	0.045
	47	45	3.93	6.31	0.042
	62	61	2.38	3.65	0.019
	80	73	13.40	3.06	0.084
CRH	21	18	4.80	11.85	0.114
	41	39	3.60	7.19	0.044
	59	55	8.50	4.06	0.072
	78	62	32.90	3.61	0.209
SRH	24	22	3.40	9.796	0.069
	40	35	7.50	7.930	0.096
	50	42	13.00	5.233	0.132
	76	64	22.70	3.473	0.149
	91	78	24.50	2.862	0.135
WO ₃	20	19	2.00	11.64	0.049
	37	35	4.00	8.086	0.054
	51	47	8.01	4.708	0.078
	62	58	8.60	3.859	0.069
	78	73	10.60	3.079	0.068

Table 4. Langmuir isotherm parameters using $\frac{1}{Q_e} = \frac{1}{Q_{max}K_L} \frac{1}{C_e} + \frac{1}{Q_{max}}$

Adsorbent	$\frac{1}{C_e}$	$\frac{1}{Q_e}$	$Q_{max}(\frac{mg}{g})$	$K_L(\frac{L}{mg})$	R_L	R^2	Note
CPS	0.066	0.689	11.037	0.009	0.992- 0.996	0.7374	<ul style="list-style-type: none"> • $0 < R_L < 1$, favorable adsorption • $R^2 > 0.70$, monolayer adsorption
	0.022	0.254					
	0.016	0.420					
	0.013	0.075					
CRH	0.053	0.208	14.684	0.021	0.954- 0.988	0.2664	<ul style="list-style-type: none"> • $0 < R_L < 1$, favorable adsorption • $R^2 < 0.70$, there are not indicating monolayer adsorption
	0.025	0.278					
	0.018	0.117					
	0.016	0.030					
SRH	0.044	0.297	11.274	0.010	0.948- 0.988	0.958	<ul style="list-style-type: none"> • $0 < R_L < 1$, favorable adsorption • $R^2 > 0.70$, monolayer adsorption
	0.028	0.133					
	0.023	0.077					
	0.015	0.044					
	0.013	0.041					
WO ₃	0.053	0.500	14.164	0.006	0.213- 0.520	0.9876	<ul style="list-style-type: none"> • $0 < R_L < 1$, favorable adsorption • $R^2 > 0.70$, monolayer adsorption
	0.028	0.250					
	0.021	0.125					
	0.017	0.116					
	0.014	0.094					

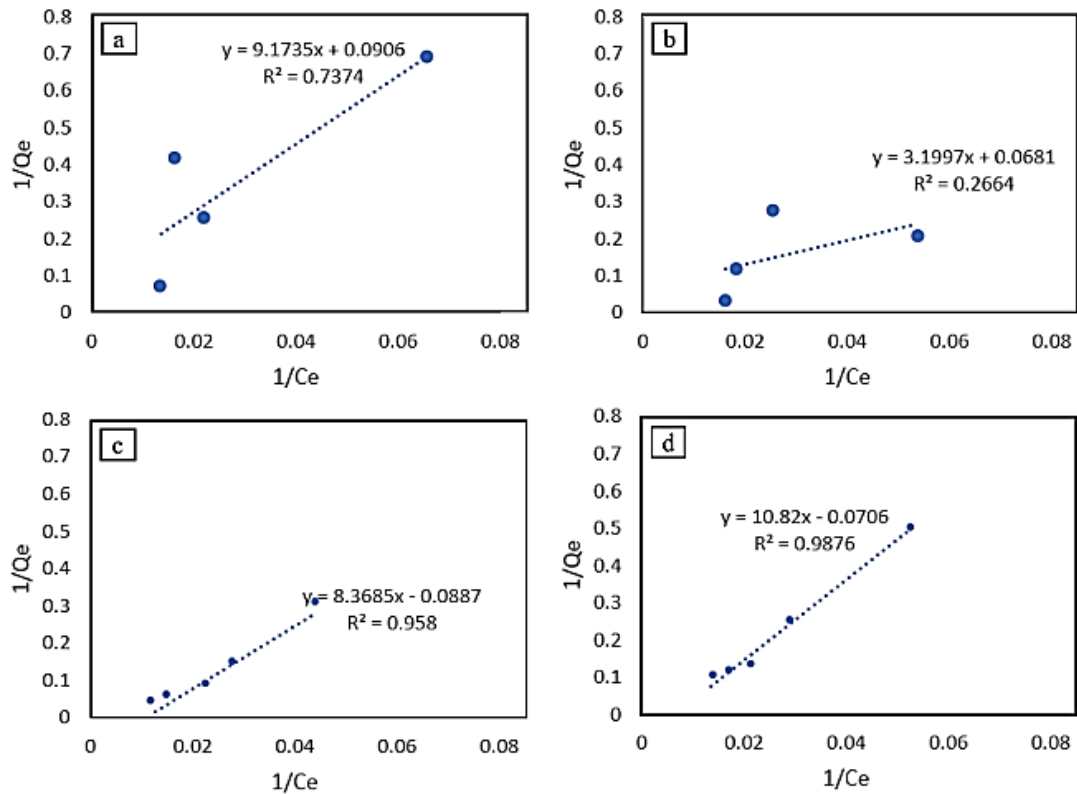


Figure 2. Langmuir isotherm model for adsorption system using a) CPS, b) CRH, c) SRH, and d) WO₃ adsorbents

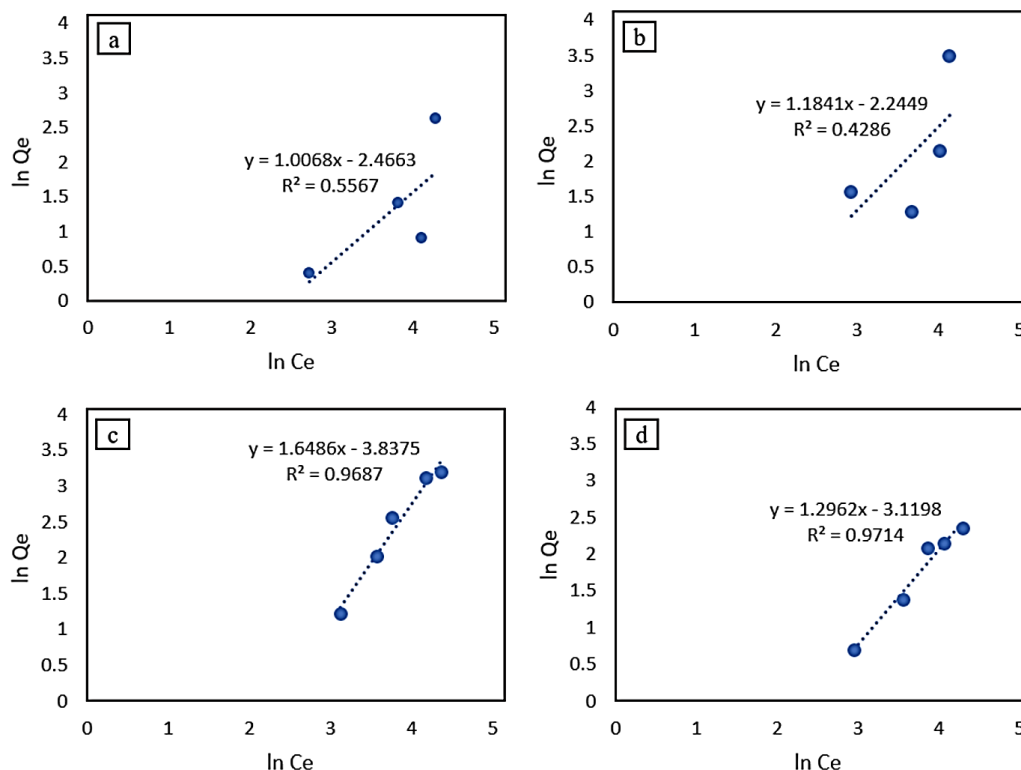
4.3.2. Freundlich

The Freundlich model adsorption parameters were obtained using **equation (3)** as presented as $\ln Q_e = \ln k_f + \frac{1}{n} \ln C_e$. To get the Freundlich model parameters, we need to convert C_e and Q_e values into the form of $\ln C_e$ and $\ln Q_e$, which are used for fitting data (see **Table 2**). The curves of data fitting result are presented in **Figures 3 (a-d)**. The result of fitting data also used to determine adsorption parameters. The result of data fitting in the form of a gradient obtained is $\frac{1}{n}$ value, and

the intercept is $\ln k_f$ value. **Table 5** shows parameter results of Freundlich model using CPS, CRH, SRH, and WO₃ adsorbents. Freundlich isotherm is good represent of SRH and WO₃ adsorption systems than CPS and CRH adsorption system, this is confirmed by the R^2 value of higher than 0.70. Thus, SRH and WO₃ adsorption system were assumed that adsorption process occurs in heterogeneous surface in multilayer form with weak adsorbate and adsorbent interaction.

Table 5. Freundlich isotherm parameters using $\ln Q_e = \ln k_f + \frac{1}{n} \ln C_e$

Adsorbent	$\ln C_e$	$\ln Q_e$	$\frac{1}{n}$	n	R^2	Note
CPS	2.723	0.371	1.0068	0.993	0.5567	<ul style="list-style-type: none"> • $\frac{1}{n} > 1$, cooperative adsorption • $n < 1$, chemical interaction between adsorbate molecules • $R^2 < 0.70$, monolayer adsorption
	3.819	1.369				
	4.121	0.867				
	4.301	2.595				
CRH	2.926	1.568	1.1841	0.844	0.4286	<ul style="list-style-type: none"> • $\frac{1}{n} > 1$, cooperative adsorption • $n < 1$, chemical interaction between adsorbate molecules • $R^2 < 0.70$, monolayer adsorption
	3.676	1.281				
	4.013	2.140				
	4.132	3.493				
SRH	3.121	1.214	1.6486	0.606	0.9687	<ul style="list-style-type: none"> • $\frac{1}{n} > 1$, cooperative adsorption • $n < 1$, chemical interaction between adsorbate molecules • $R^2 > 0.70$, multilayer adsorption
	3.567	2.015				
	3.758	2.565				
	4.172	3.122				
WO ₃	2.945	0.693	1.2962	0.771	0.9714	<ul style="list-style-type: none"> • $\frac{1}{n} > 1$, cooperative adsorption • $n < 1$, chemical interaction between adsorbate molecules • $R^2 > 0.70$, multilayer adsorption
	3.556	1.386				
	3.865	2.080				
	4.065	2.152				
	4.293	2.361				

**Figure 3.** Freundlich isotherm model for adsorption system using a) CPS, b) CRH, c) SRH, and d) WO₃ adsorbents

4.3.3. Temkin

Temkin model parameters were obtained using **equation (4)** as presented as $q_e = B_T \ln A_T + B_T \ln C_e$. To get the Temkin model parameters, we need to convert C_e and Q_e values into the forms of $\ln C_e$ and Q_e , which are used for data fitting (see **Table 2**). The curves of data fitting result are presented in **Figures 4 (a-d)**. The result of fitting data also used to determine adsorption parameter. The result of data fitting in the form of a gradient obtained is the B value to calculate B_T value and the intercept is the $B_T \ln A_T$ value. **Table 6** shows parameter results of Temkin model using CPS, CRH, SRH, and WO_3 adsorbents. A_T value in **Table 6** is the Temkin equilibrium constant corresponding to the maximum binding energy where the high A_T shows attractive interaction between adsorbate-adsorbent system. The A_T value for all adsorption systems shows a relatively small value means less affinity between the adsorbent and adsorbate molecules since there are physical interaction dominate that confirmed by B_T parameter. Physical interaction only involves more interaction weak, for example in the form of adsorbate polarization with adsorbent. Base on correlation coefficient value ($R^2 > 0.70$), SRH and WO_3 are suitable with Temkin isotherm, while CPS and CRH adsorption system are not suitable. Temkin isotherm informs that adsorption is characterized by uniform distribution adsorbate to adsorbent surface.

4.3.4. Dubinin-Radushkevich

Dubinin-Radushkevich model adsorption parameters were obtained using **equation (5)** as follow as $\ln q_e = \ln q_s - (\beta \epsilon^2)$. To get the Dubinin-Radushkevich model parameters, we need to convert Q_e into the form of $\ln Q_e$ value and looking for the ϵ^2 value which are used for data fitting (see **Table 2**). The curves of data fitting result are presented in **Figures 5 (a-d)**. The result of data fitting also used to determine adsorption parameter. The result of data fitting in the form of a gradient obtained is the β value to calculate E value. **Table 7** shows parameter

results of Dubinin-Radushkevich using CPS, CRH, SRH, and WO_3 adsorbents. Parameter β in **Table 7** is Dubinin-Radushkevich isotherm constant related saturation capacity. High β value shows high adsorption capacity. Based on β parameter, WO_3 has higher β value while CRH has smaller β value than others. β value influenced by pore volume. The larger pore volume impact on highest maximum binding energy value. Plotting data of Dubinin-Radushkevich show that SRH and WO_3 adsorption system have the best correlation coefficient since correlation coefficient value is high ($R^2 > 0.70$). Thus, SRH and WO_3 adsorption system are considered by Dubinin-Radushkevich have adsorbent size proportional to the micropore size.

4.3.5. Jovanovic

Jovanovic model adsorption parameters were obtained using **equation (8)** as presented as $\ln q_e = \ln q_{max} - K_j C_e$. To get the Jovanovic model parameters, we need C_e data and we need to convert Q_e into the form of $\ln Q_e$ which are used for data fitting (see **Table 2**). The curves of fitting data are presented in **Figures 6 (a-d)**. The result of fitting data also used to determine adsorption parameter. The result of data fitting in the form of a gradient obtained is the K_j value and intercept is the $\ln Q_{max}$ value. **Table 8** shows parameters of Jovanovic using CPS, CRH, SRH, and WO_3 adsorbents. K_j and Q_{max} in **Table 8** are the Jovanovic constant and the maximum uptake of adsorbate molecule. Q_{max} related with how much adsorbates are absorbed by a particular adsorbent where the higher Q_{max} value shows better adsorbent capacity. CRH and SRH adsorbents showed identically small adsorption capacity (Q_{max}) value as well as CPS and WO_3 . Based on Dubinin-Radushkevich isotherm, WO_3 and CPS adsorbent shows high adsorption capacity. This condition is possible due to surface active site is efficient in adsorbing the adsorbate molecule although it has small

surface area and pore. The Jovanovic isotherm reflects well the entire adsorption system (i.e., CPS, CRH, SRH, and WO₃) which is shown from the relatively high correlation

coefficient value of each adsorption system ($R^2 > 0.70$). Compatibility with Jovanovic's model indicates that there is existence of monolayer adsorption.

Table 6. Temkin isotherm parameters using $q_e = B_T \ln A_T + B_T \ln C_e$

Adsorbent	$\ln C_e$	Q_e	$A_T \left(\frac{L}{g}\right)$	$B_T \left(\frac{J}{mol}\right)$	R^2	Note
CPS	2.723	1.45	0.025	144.97	0.4851	<ul style="list-style-type: none"> • $B_T < 8 \text{ kJ/mol}$, physical interaction between adsorbate molecules • $R^2 < 0.70$, no uniform distribution adsorbate to adsorbent surface
	3.819	3.93				
	4.121	2.38				
	4.301	13.40				
CRH	2.926	4.80	0.026	46.528	0.6465	<ul style="list-style-type: none"> • $B_T < 8 \text{ kJ/mol}$, physical interaction between adsorbate molecules • $R^2 < 0.70$, no uniform distribution adsorbate to adsorbent surface
	3.676	3.60				
	4.013	8.50				
	4.132	32.90				
SRH	3.121	3.40	0.038	99.573	0.9973	<ul style="list-style-type: none"> • $B_T < 8 \text{ kJ/mol}$, physical interaction between adsorbate molecules • $R^2 > 0.70$, uniform distribution adsorbate to adsorbent surface
	3.567	7.50				
	3.758	13.00				
	4.172	22.70				
	4.367	24.50				
WO ₃	2.945	2.00	0.045	264.64	0.9216	<ul style="list-style-type: none"> • $B_T < 8 \text{ kJ/mol}$, physical interaction between adsorbate molecules • $R^2 > 0.70$, uniform distribution adsorbate to adsorbent surface
	3.556	4.00				
	3.865	8.01				
	4.065	8.60				
	4.293	10.60				

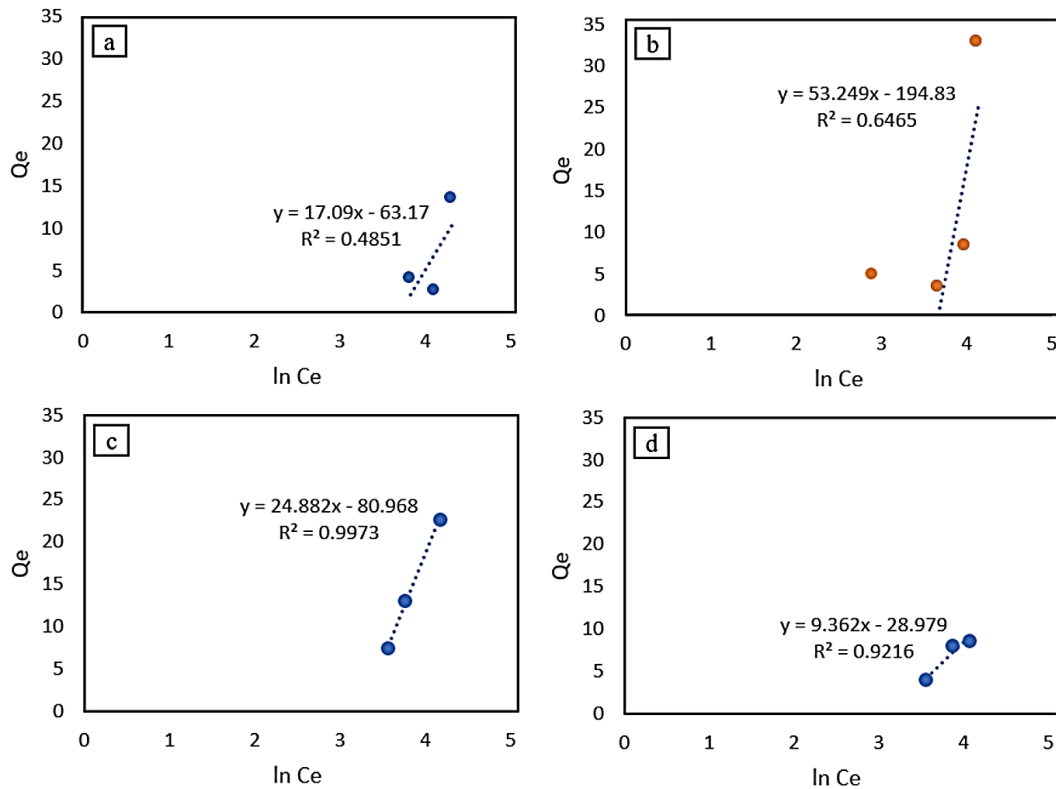


Figure 4. Temkin isotherm model for adsorption system using a) CPS, b) CRH, c) SRH, and d) WO_3 adsorbents

4.3.6. Halsey

Halsey model adsorption parameters were obtained using **equation (9)** as presented as $\ln Q_e = \frac{1}{n_H} \ln K_H - \frac{1}{n} \ln C_e$. To get the Halsey model parameters, we need to convert C_e and Q_e data into the form of $\ln C_e$ and $\ln Q_e$, which are used for data fitting (see **Table 2**). The curves of data fitting result are presented in **Figures 7 (a-d)**. The result of data fitting also used to determine the adsorption parameter. The result of data fitting in the form of a gradient obtained is the $\frac{1}{n}$ value and intercept is the $\frac{1}{n} \ln K_H$ value.

Table 9 shows parameter results of Halsey using CPS, CRH, SRH, and WO_3 adsorbents. K_H and n in **Table 9** are the Halsey isotherm constants. Halsey isotherm reflect good adsorption system for SRH and WO_3 since ($R^2 > 0.70$) is relatively high. While, CPS and CRH adsorption system are not suitable with Halsey isotherm. Compatibility with Halsey model due to high R^2 indicates that there is existence of multilayer adsorption. From Halsey's parameter, we can identify that the higher the adsorption capacity (Q_e) correlates with the increase in the value of n .

Table 7. Dubinin-Radushkevich isotherm parameters $\ln q_e = \ln q_s - (\beta \varepsilon^2)$

Adsorbent	$\ln Q_e$	ε^2	$\beta \left(\frac{\text{mol}^2}{\text{kJ}^2} \right)$	$E \left(\frac{\text{kJ}}{\text{mol}} \right)$	R^2	Note
CPS	0.371	14.43	3.88328	0.358	0.4996	<ul style="list-style-type: none"> • $E < 8 \text{ kJ/mol}$, physical interaction between adsorbate molecules • $R^2 < 0.70$, no micropore size is exist in adsorbent surface
	1.369	6.31				
	0.867	3.65				
	2.595	3.06				
CRH	1.568	11.85	2.6092	0.438	0.455	<ul style="list-style-type: none"> • $E < 8 \text{ kJ/mol}$, physical interaction between adsorbate molecules • $R^2 < 0.70$, no micropore size is exist in adsorbent surface
	1.281	7.19				
	2.140	4.06				
	3.493	3.61				
SRH	1.214	9.796	3.5364	0.376	0.9829	<ul style="list-style-type: none"> • $E < 8 \text{ kJ/mol}$, physical interaction between adsorbate molecules • $R^2 > 0.70$, micropore size is exist in adsorbent surface
	2.015	7.930				
	2.565	5.233				
	3.122	3.473				
	3.199	2.862				
WO ₃	0.693	11.64	5.1626	0.311	0.9976	<ul style="list-style-type: none"> • $E < 8 \text{ kJ/mol}$, physical interaction between adsorbate molecules • $R^2 > 0.70$, micropore size is exist in adsorbent surface
	1.386	8.086				
	2.080	4.708				
	2.152	3.859				
	2.361	3.079				

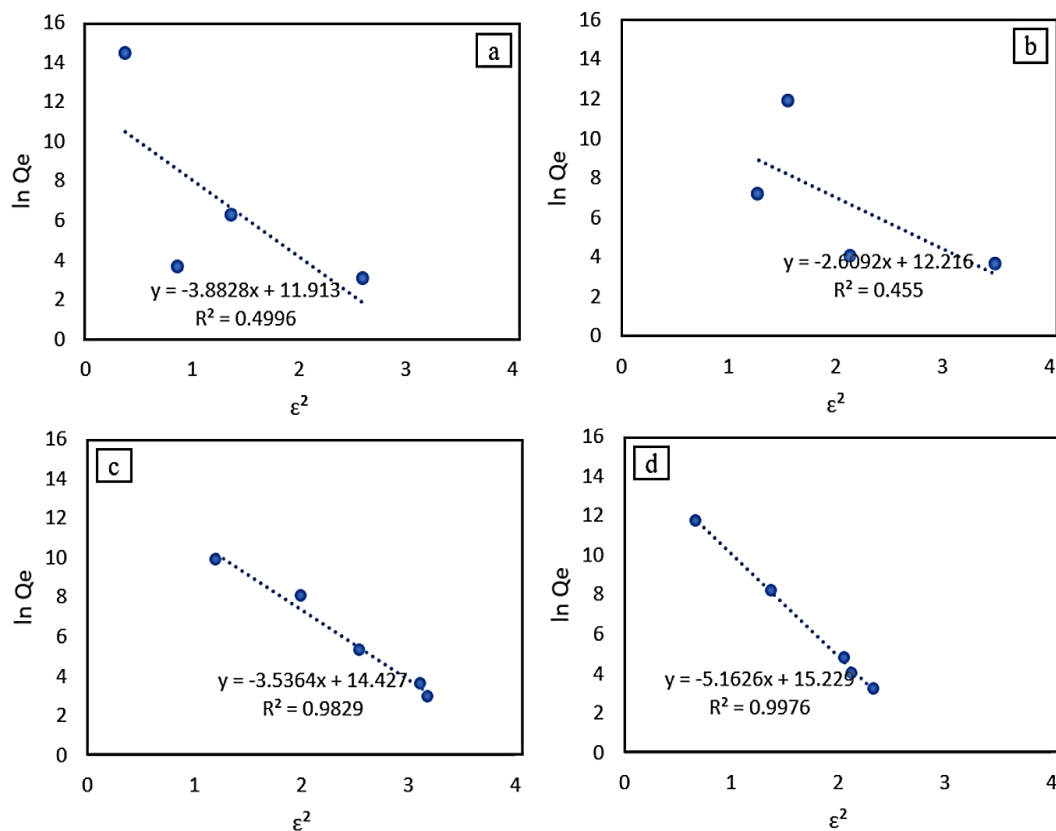
**Figure 5.** Dubinin-Radushkevich isotherm model for adsorption system using a) CPS, b) CRH, c) SRH, and d) WO₃ adsorbents

Table 8. Jovanovic isotherm parameter using $\ln q_e = \ln q_{max} - K_J C_e$

Adsorbent	C_e	$\ln Q_e$	$K_J \left(\frac{L}{mg}\right)$	$q_{max} \left(\frac{mg}{g}\right)$	R^2	Note
CPS	15	0.371	0.3331	1.508	0.936	$R^2 > 0.70$, the existence of monolayer on the surface of adsorbent
	47	1.369				
	62	0.867				
	73	2.595				
CRH	18	1.568	0.139	3.502	0.9526	$R^2 > 0.70$, the existence of monolayer on the surface of adsorbent
	39	1.281				
	55	2.140				
	62	3.493				
SRH	22	1.214	0.1727	3.294	0.9357	$R^2 > 0.70$, the existence of monolayer on the surface of adsorbent
	35	2.015				
	42	2.565				
	64	3.122				
WO ₃	19	0.693	0.3755	1.614	0.9602	$R^2 > 0.70$, the existence of monolayer on the surface of adsorbent
	35	1.386				
	47	2.080				
	58	2.152				
	73	2.361				

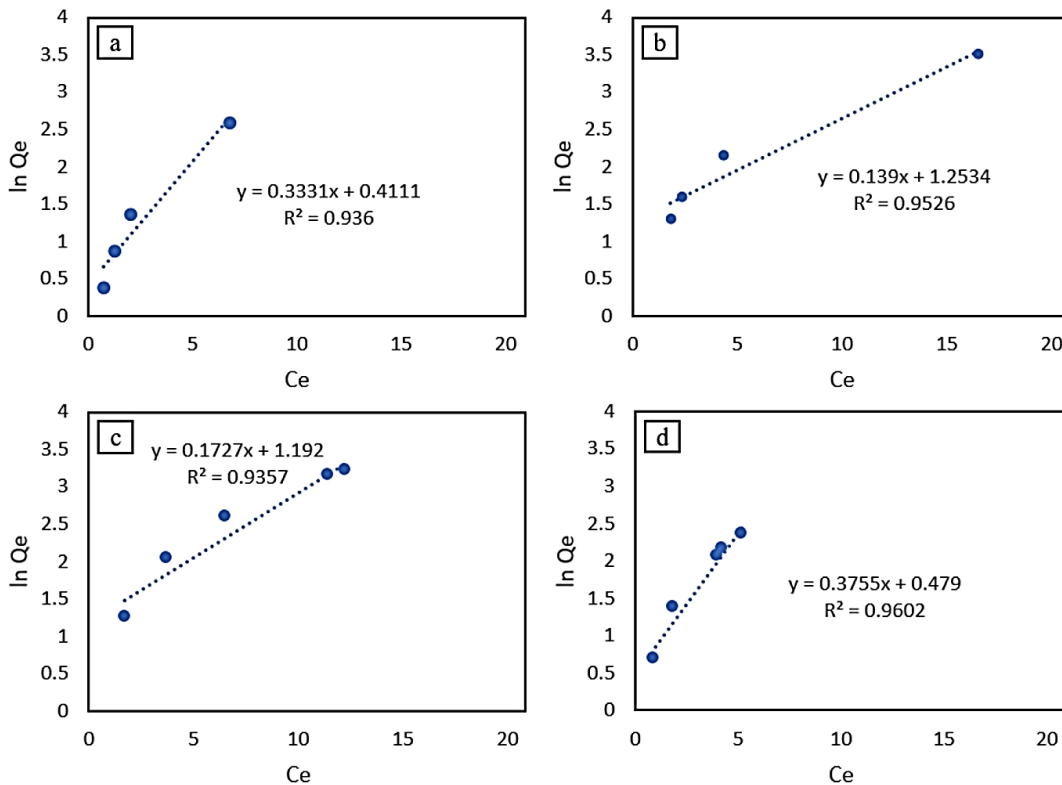


Figure 6. Jovanovic isotherm model for adsorption system using a) CPS, b) CRH, c) SRH, and d) WO₃ adsorbents

Table 9. Halsey isotherm parameters using $\ln Q_e = \frac{1}{n_H} \ln K_H - \frac{1}{n} \ln C_e$

Adsorbent	$\ln C_e$	$\ln Q_e$	$\frac{1}{n}$	n	K_H	R^2	Note
CPS	2.723	0.371	1.0068	0.992	0.086	0.5567	$R^2 < 0.70$, the existence of monolayer on the surface of adsorbent
	3.819	1.369					
	4.121	0.867					
	4.301	2.595					
CRH	2.926	1.568	1.1841	0.844	0.150	0.4286	$R^2 < 0.70$, the existence of monolayer on the surface of adsorbent
	3.676	1.281					
	4.013	2.140					
	4.132	3.493					
SRH	3.121	1.214	1.6486	0.607	0.097	0.9687	$R^2 > 0.70$, the existence of multilayer on the surface of adsorbent
	3.567	2.015					
	3.758	2.565					
	4.172	3.122					
WO ₃	2.945	0.693	1.2962	0.771	0.090	0.9714	$R^2 > 0.70$, the existence of multilayer on the surface of adsorbent
	3.556	1.386					
	3.865	2.080					
	4.293	2.361					

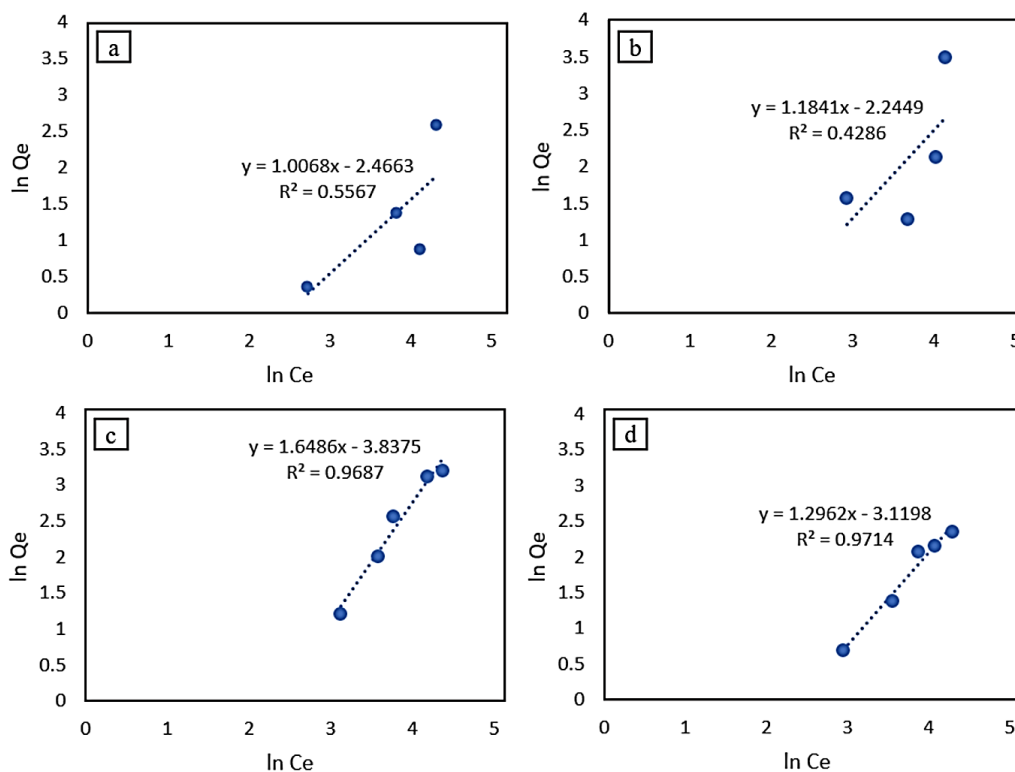


Figure 7. Halsey isotherm model for adsorption system using a) CPS, b) CRH, c) SRH, and d) WO₃ adsorbents

4.3.7. Harkin-Jura

Harkin-Jura model adsorption parameters were obtained using **equation (10)** as presented as $\frac{1}{q_e^2} = \frac{B}{A} - \left(\frac{1}{A}\right) \log C_e$. To get the Harkin-Jura model parameters, we need to convert C_e and Q_e data into the form of $\log C_e$ and $\frac{1}{q_e^2}$ which are used for data fitting (see **Table 2**). The curves of data fitting result are presented in **Figures 8 (a-d)**. The result of data fitting also used to determine adsorption parameter. The result of data fitting in the form of a gradient obtained is the $\frac{1}{A_H}$ value and intercept is the $\frac{B_H}{A_H}$ value. **Table 10** shows parameter results of Harkin-Jura using CPS, CRH, SRH, and WO_3

adsorbents. B and A in **Table 10** are Harkin-Jura constants. Based on R^2 adsorption using CPS, SRH, WO_3 adsorbent is suitable since $R^2 > 0.70$. From the Harkin-Jura parameter, we can identify that the higher values of parameters of A_{HJ} and β_{HJ} , the worse the adsorption capacity (Q_e). The Harkin-Jura model also explains the theoretical surface area by using equation (12) as presented as $S^2 = -\frac{\beta \times 4.606RTN}{q}$. For example, if we use the assumption of q value of carbon, silica, and WO_3 as in **Table 1**, and the temperature used is room temperature (298 K), then the surface area value is presented in **Table 11**.

Table 10. Harkin-Jura isotherm parameters using $\frac{1}{q_e^2} = \frac{B}{A} - \left(\frac{1}{A}\right) \log C_e$

Adsorbent	$\log C_e$	$1/q_e^2$	slope	intercept	β_{HJ}	A_{HJ}	R^2	Note
CPS	1.183	0.476	-0.6275	1.2003	1.593	1.912	0.85	$R^2 > 0.70$, the existence of multilayer on the surface of adsorbent
	1.659	0.065						
	1.790	0.176						
	1.868	0.005						
CRH	1.270	0.043	-0.0754	0.1545	13.262	0.1545	0.2747	$R^2 < 0.70$, the existence of monolayer on the surface of adsorbent
	1.596	0.077						
	1.743	0.014						
	1.795	0.001						
SRH	1.355	0.088	-0.1469	0.2654	6.807	0.3654	0.7261	$R^2 > 0.70$, the existence of multilayer on the surface of adsorbent
	1.549	0.018						
	1.632	0.006						
	1.812	0.002						
	1.897	0.002						
WO_3	1.279	0.250	-0.4226	0.7575	2.366	0.7575	0.8704	$R^2 > 0.70$, the existence of multilayer on the surface of adsorbent
	1.544	0.062						
	1.679	0.015						
	1.766	0.013						
	1.864	0.009						

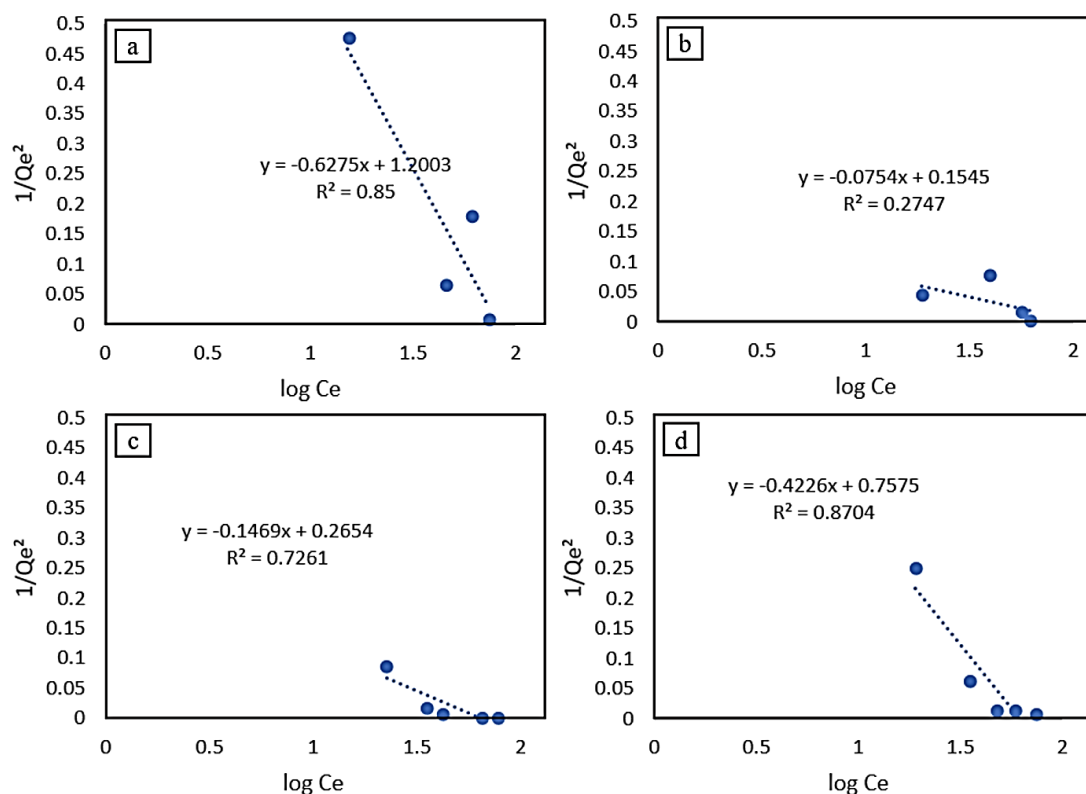


Figure 8. Harkin-Jura isotherm model for adsorption system using a) CPS, b) CRH, c) SRH, and d) WO₃ adsorbent

Table 11. Calculation of the surface area with the Harkin-Jura model using equations $S^2 = \frac{\beta \times 4.606RTN}{q}$

Adsorbent	β	$4.606RTN$	$S(\frac{m^2}{g})$
CPS	1.593	2.3060×10^2	1000
CRH	13.262	2.3060×10^{24}	3000
SRH	6.807	2.3060×10^{24}	370
WO ₃	2.366	2.3060×10^{24}	37

4.3.8. Flory-Huggins

Flory-Huggins model adsorption parameters were obtained using equation (11) as presented as $\log \frac{\theta}{C_e} = \log K_{FH} + n \log(1 - \theta)$. To get the Flory-Huggins model parameters, we need to convert θ data into the form of $\log \frac{\theta}{C_0}$ and $\log(1 - \theta)$ and which are used for data fitting (see Table 2). The

curves of data fitting result are presented in Figures 9 (a-d). The result of data fitting also used to determine adsorption parameter. The result of data fitting in the form of a gradient obtained is the n_{FH} value and intercept is the $\log K_{FH}$ value. Table 12 shows parameter results of Flory-Huggins using CPS, CRH, SRH, and WO₃ adsorbents. K_{FH} in Table

12 are the number of adsorbates occupying adsorption sites and the Flory-Huggins constant. Adsorbent SRH and WO₃ have good K_{FH} value than CPS and CRH. This condition showed SRH and WO₃ have better adsorbent-adsorbate interaction. Moreover, SRH and

WO₃ form multilayer adsorption which makes the adsorbate more attached to the adsorbent due to chemical bonds. Fowler-Huggins is poor suitable with all adsorption system (i.e., CPS, CRH, SRH, and WO₃) because $R^2 < 0.70$.

Table 12. Flory-Huggins isotherm parameters using $\log \frac{\theta}{C_e} = \log K_{FH} + n \log(1 - \theta)$

Adsorbent	$\log(1 - \theta)$	$\log \frac{\theta}{C_i}$	n_{FH}	K_{FH} (L/mg)	ΔG°	R^2	Note
CPS	-0.020	-2.541	-0.014	0.863	2138	0.2068	<ul style="list-style-type: none"> • $\Delta G^\circ > 0$, not spontaneously adsorption • $n_{FH} < 1$, represent more than one active adsorbent zone occupied by the adsorbate • $R^2 < 0.70$, the existence of monolayer on the surface of adsorbent
	-0.018	-3.056					
	-0.008	-3.516					
	-0.038	-2.982					
CRH	-0.052	-2.265	-0.0604	0.611	2155	0.3038	<ul style="list-style-type: none"> • $\Delta G^\circ > 0$, not spontaneously adsorption • $n_{FH} < 1$, more than one active adsorbent zone occupied by the adsorbate • $R^2 < 0.70$, the existence of monolayer on the surface of adsorbent
	-0.019	-2.975					
	-0.032	-2.919					
	-0.101	-2.576					
SRH	-0.031	-2.547	0.0874	1.507	3733	0.3992	<ul style="list-style-type: none"> • $\Delta G^\circ > 0$, not spontaneously adsorption • $n_{FH} < 1$, more than one active adsorbent zone occupied by the adsorbate • $R^2 < 0.70$, the existence of monolayer on the surface of adsorbent
	-0.044	-2.611					
	-0.062	-2.572					
	-0.070	-2.708					
	-0.062	-2.829					
WO ₃	-0.022	-2.605	0.0184	1.056	3731	0.3267	<ul style="list-style-type: none"> • $\Delta G^\circ > 0$, not spontaneously adsorption • $n_{FH} < 1$, more than one active adsorbent zone occupied by the adsorbate • $R^2 < 0.70$, the existence of monolayer on the surface of adsorbent
	-0.023	-2.839					
	-0.035	-2.820					
	-0.031	-2.955					
	-0.030	-3.062					

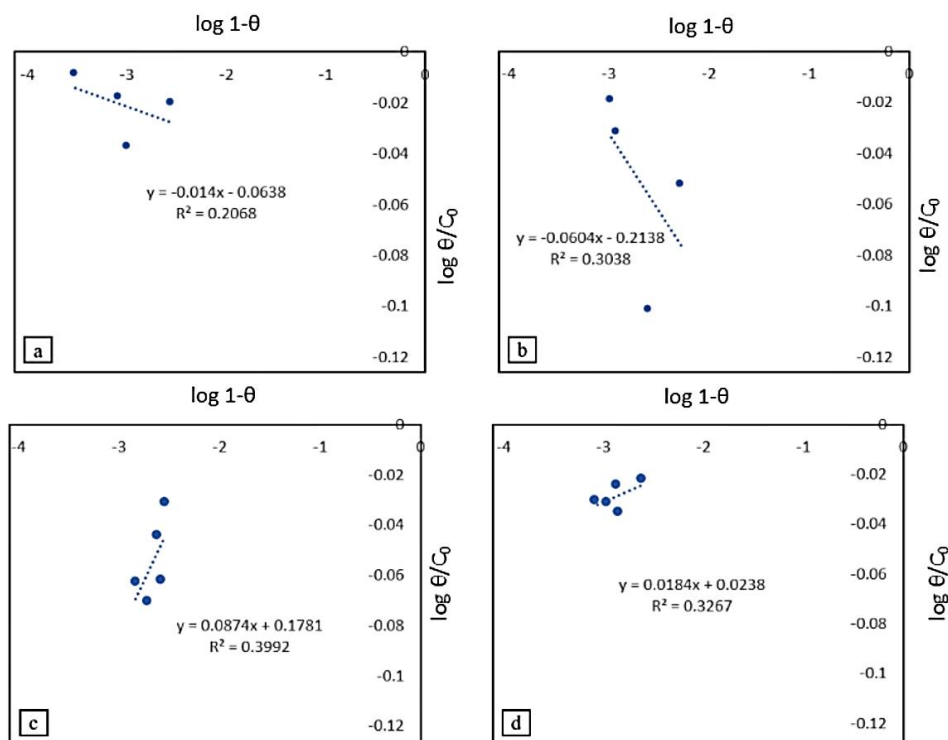


Figure 9. Flory-Huggins isotherm model for adsorption system using a) CPS, b) CRH, c) SRH, and d) WO_3 adsorbents

4.3.9. Fowler-Guggenheim

Fowler-Guggenheim model adsorption parameters were obtained using **equation (13)** as presented as $\ln\left(\frac{C_e(1-\theta)}{\theta}\right) - \frac{\theta}{1-\theta} = -\ln K_{FG} + \frac{2W\theta}{RT}$. To get the Fowler-Guggenheim model parameters, we need to plot θ vs $\ln\frac{C_e(1-\theta)}{\theta}$ data (see **Table 2**). The curves of data fitting result are presented in **Figures 10 (a-d)**. The result of data fitting also used to determine adsorption parameter. The result of data fitting in the form of a gradient obtained is the $\frac{2W\theta}{RT}$ value and intercept is the $\ln K_{FG}$ value. **Table 13** shows parameter results of Fowler-

Guggenheim using CPS, CRH, SRH, and WO_3 adsorbents. K_{FG} in **Table 13** is Fowler-Guggenheim constant represent adsorbent-adsorbate interaction. Higher K_{FG} value indicates a good interaction between adsorbent-adsorbate. All adsorbent system shows identically small K_{FG} value means weak interaction adsorbent-adsorbate since there are surface active site is less efficient in adsorbing the adsorbate molecules due to domination of physical interaction. Fowler-Guggenheim is poor suitable with all adsorption system (i.e., CPS, CRH, SRH, and WO_3) because $R^2 < 0.70$.

Table 13. Fowler Guggenheim isotherm parameters using $\ln\left(\frac{C_e(1-\theta)}{\theta}\right) - \frac{\theta}{1-\theta} = -\ln K_{FG} + \frac{2W\theta}{RT}$

Adsorbent	$\ln \frac{C_e(1-\theta)}{\theta}$	θ	K_{FG} (L/mg)	W (kJ/mol)	R^2	Note
CPS	5.757	0.045	4×10^{-4}	-23403	0.2599	<ul style="list-style-type: none"> $W < 0$ kJ/mol, repulsive interaction between adsorbed molecule $R^2 < 0.70$, the existence of monolayer on the surface of adsorbent
	6.952	0.042				
	8.058	0.019				
	6.692	0.084				
CRH	4.973	0.114	1×10^{-3}	-11595	0.4814	<ul style="list-style-type: none"> $W < 0$ kJ/mol, repulsive interaction between adsorbed molecule $R^2 < 0.70$, the existence of monolayer on the surface of adsorbent
	6.761	0.044				
	6.572	0.072				
	5.464	0.209				
SRH	5.722	0.069	3×10^{-3}	4028	0.1738	<ul style="list-style-type: none"> $W < 0$ kJ/mol, repulsive interaction between adsorbed molecule $R^2 < 0.70$, the existence of monolayer on the surface of adsorbent
	5.811	0.096				
	5.639	0.132				
	5.912	0.149				
	6.226	0.135				
WO ₃	5.897	0.049	4×10^{-3}	22437	0.28	<ul style="list-style-type: none"> $W < 0$ kJ/mol, repulsive interaction between adsorbed molecule $R^2 < 0.70$, the existence of monolayer on the surface of adsorbent
	6.427	0.054				
	6.332	0.078				
	6.661	0.069				
	6.910	0.068				

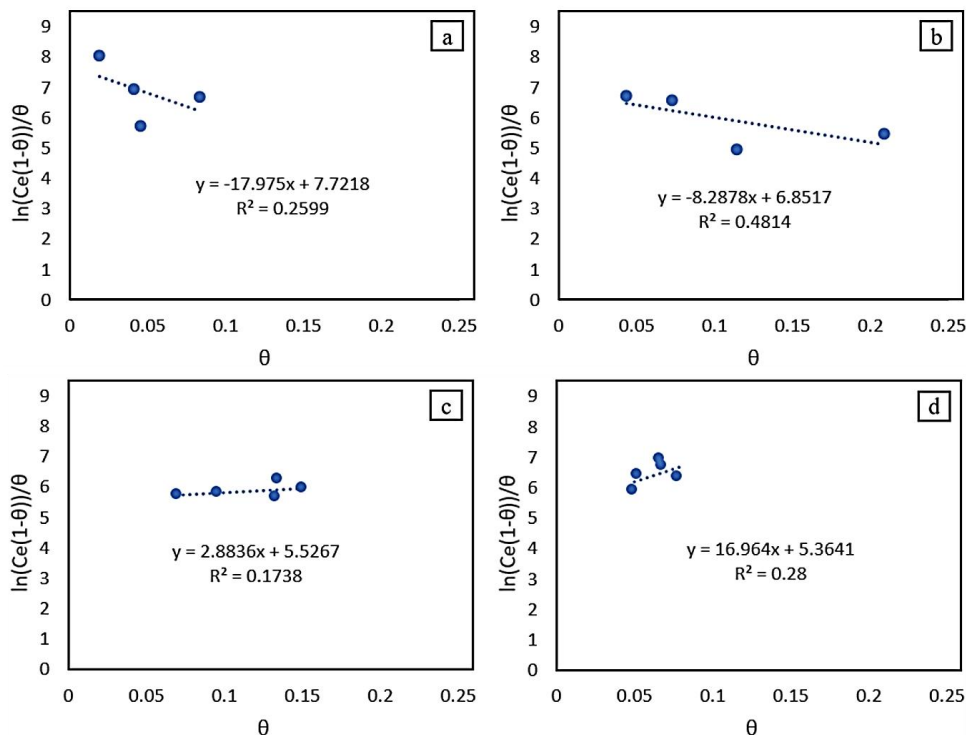


Figure 10. Fowler-Guggenheim isotherm model for adsorption system using a) CPS, b) CRH, c) SRH, and d) WO₃ Adsorbents

4.3.10. Hill-Deboer

Hill-Deboer model adsorption parameters were obtained using **equation (14)** as presented as $\ln \left[\frac{C_e(1-\theta)}{\theta} \right] - \frac{\theta}{1-\theta} = -\ln K_1 - \frac{K_2\theta}{RT}$. To get the Hill-Deboer model parameters, we need to plot θ vs $\ln \frac{C_e(1-\theta)}{\theta} - \frac{\theta}{1-\theta}$ data. The curves of data fitting result are presented in **Figures 11 (a-d)**. The result of fitting data also used to determine adsorption parameter. The result of data fitting in the form of a gradient obtained is the $\frac{K_2\theta}{RT}$ value and intercept is the $\ln K_1$ value. **Table 14** shows parameter results of a Hill-Deboer using CPS, CRH, SRH, and WO_3 adsorbents. K_1 in **Table 14** is the Hill-Deboer constant interaction between adsorbent and adsorbate. Higher K_1 value indicates a good interaction between adsorbent-adsorbate. However, all adsorbents system indicate a small value of K_1 means poor interaction between adsorbent-adsorbate since active site is not effective in carrying out adsorption process. Hill-Deboer is poor suitable with all adsorption system (i.e., CPS, CRH, SRH, and WO_3) because $R^2 < 0.70$.

4.4. Approximately Isotherm Model

The experimental data of the adsorption process in **Table 2** were analyzed through regression analysis to match the linear correlation of the adsorption isotherm mathematical models. Fitting data based on the plotted way in **Table 1** for each adsorption model is used to determine the adsorption parameters that correspond to each adsorption model. The parameters obtained after the data fitting process are summarized in **Tables 3-12. Figures 2-11**

present the plotting of the experimental results.

Figures 2 (a-d) show the fitting data based on the Langmuir adsorption isotherm. The Langmuir isotherm for the study of the adsorption of curcumin solution with the and CRH show poor adsorption characteristics because it gives a low correlation coefficient value ($R^2 < 1$) is too far closer to the 0.90. Meanwhile, adsorption of CPS, SRH, and WO_3 adsorbents matches the Langmuir model with a coefficient correlation ($R^2 > 0.90$). This means that the adsorption system using CRH does not allow monolayer formation. However, the reverse phenomenon is for the adsorption system using cps, SRH, and WO_3 adsorbents. The analysis of the separation factor (R_L) shows R_L value in the range between 0 and 1 for all cases which indicates that the adsorption process has favorable adsorption characteristics.

Figures 3 (a-d) show the Freundlich isotherm curve. Freundlich isotherm curve shows very small correlation coefficient value for adsorption system using CPS and CRH adsorbent compared to adsorption system with SRH and WO_3 adsorbent. This model suggests that the adsorption system with SRH and WO_3 fits into the Freundlich model, which allows the formation of a multilayer structure.

Figures 4 (a-d) are the linear curve of the Temkin adsorption. The adsorption system with CPS and CRH adsorbents does not match with the Temkin model isotherm because the R^2 value is less than 0.90. While, the adsorption system with SRH and WO_3 adsorbents are compatible with Temkin isotherm model.

Table 14. Hill-Deboer isotherm parameters using $\ln \left[\frac{C_e(1-\theta)}{\theta} \right] - \frac{\theta}{1-\theta} = -\ln K_1 - \frac{K_2\theta}{RT}$

Adsorbent	$\ln \frac{C_e(1-\theta)}{\theta} - \frac{\theta}{1-\theta}$	θ	K_1 (L/mg)	K_2 (kJ/mol)	R^2	Note
CPS	5.709	0.045	4	-49716	0.284	<ul style="list-style-type: none"> • $K_2 < 0$ kJ/mol, repulsive interaction between adsorbate molecules • $R^2 < 0.70$, the existence of monolayer on the surface of adsorbent
	6.901	0.042	$\times 10^{-4}$			
	8.038	0.019				
	6.600	0.084				
CRH	4.844	0.114	1	-26919	0.5589	<ul style="list-style-type: none"> • $K_2 < 0$ kJ/mol, repulsive interaction between adsorbate molecules • $R^2 < 0.70$, the existence of monolayer on the surface of adsorbent
	6.715	0.044	$\times 10^{-3}$			
	6.494	0.072				
	5.199	0.209				
SRH	5.647	0.069	3	4535	0.0625	<ul style="list-style-type: none"> • $K_2 < 0$ kJ/mol, attractive interaction between adsorbate molecules • $R^2 < 0.70$, the existence of monolayer on the surface of adsorbent
	5.704	0.096	$\times 10^{-3}$			
	5.487	0.132				
	5.736	0.149				
	6.071	0.135				
WO₃	5.845	0.049	4	41858	0.2527	<ul style="list-style-type: none"> • $K_2 < 0$ kJ/mol, attractive interaction between adsorbate molecules • $R^2 < 0.70$, the existence of monolayer on the surface of adsorbent
	6.370	0.054	$\times 10^{-3}$			
	6.247	0.078				
	6.587	0.069				
	6.838	0.068				

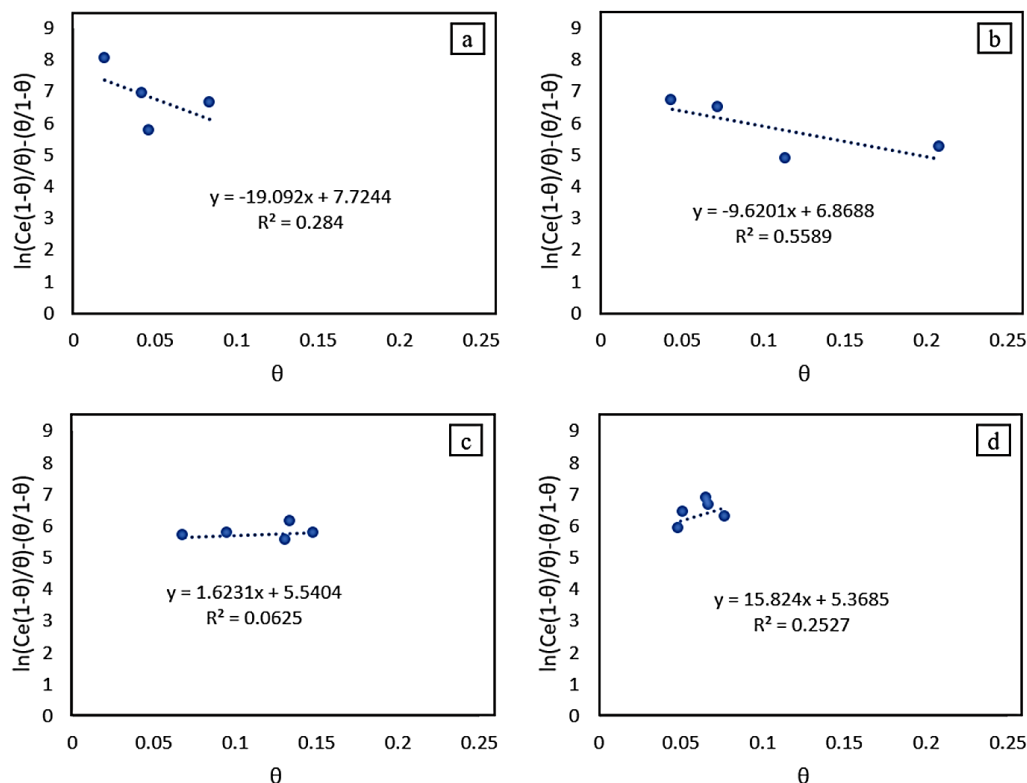


Figure 11. Hill-Deboer isotherm model for adsorption system using a) CPS, b) CRH, c) SRH, and d) WO₃ adsorbents

Figures 5 (a-d) are an analysis fitting based on the Dubinin-Radushkevich model. Based on the correlation coefficient value, the adsorption system with SRH and WO₃ adsorbents are compatible with the Dubinin-Radushkevich model, whereas the adsorption system with CPS and CRH adsorbents does not. Therefore, the adsorption system with CPS and CRH adsorbents was not well reflected by the Dubinin-Radushkevich isotherm model. The Dubinin-Radushkevich isotherm reflects a good fit for the SRH and WO₃ adsorbent.

Figures 6 (a-d) are the isotherm curve of the Jovanovic model. Based on the analysis of the coefficient correlation value, the Jovanovic isotherm model is the most suitable and most reflective of all cases of adsorption systems because the value of $R^2 > 0.9$.

Figures 7 (a-d) are an analysis fitting based on the Halsey model. The adsorption system

that is most suitable for this model is the adsorption system with SRH and WO₃ adsorbents. Meanwhile, the Halsey model is not suitable in representing the adsorption system with CPS and CRH.

Figures 8 (a-d) show the fitting analysis using the Harkin-Jura adsorption isotherm. The adsorption system with CPS and CRH adsorbent are the least suitable because the R^2 value is < 0.9 . The incompatibility with the Harkin-Jura isotherm represents that the adsorption process does not follow a multilayer adsorption model. On the other hand, the Harkin-Jura isotherm is compatible with the adsorption system with SRH, and WO₃ adsorbents because the R^2 value is close to 0.9 which allows the formation of multilayers on the adsorbent surface.

Figures 9 (a-d), 10 (a-d), and 11 (a-d) are the results of fitting data based on the Flory Huggins, Fowler Guggenheim, and Hill-Deboer models. These three models show poor correlation coefficient values for all

adsorption cases (i.e., CPS, CRH, SRH, and WO_3), meaning that they reflect an adsorption system that is not suitable for all cases.

5. Discussion

Based on the R^2 value for each adsorption model, the adsorption system in CPS is compatible with Langmuir, Harkin-Jura, and Jovanovic isotherm models. CRH adsorbents is only compatible with the Jovanovic model. Langmuir and Jovanovic model have same assumption that adsorption process occurs by forming a monolayer structure without the presence of adsorbate-adsorbent lateral interactions for CPS and CRH adsorbents (Ayawei *et al.*, 2017). Besides assuming the adsorption is monolayer, the adsorption system with the CPS adsorbent is also assumed to have adsorption by forming a multilayer. This is confirmed because it fits the Harkin-Jura model.

For adsorption systems with SRH and WO_3 adsorbents, both of them are incompatible with the Harkin Jura, Flory Huggins, Fowler Guggenheim, and Hill-Deboer models. Meanwhile, the other six models are suitable. The adsorption system with the SRH adsorbent followed suit with the order of the Temkin > Dubinin-Radushkevich > Freundlich > Halsey > Langmuir > Jovanovic models. Meanwhile, the order of compatibility of the adsorption system with the WO_3 adsorbent is summarized as follows Dubinin Radushkevich > Langmuir > Freundlich > Halsey > Jovanovic > Temkin models. The adsorption system with SRH and WO_3 adsorbents has a good correlation with the Langmuir model informing the monolayer adsorption process, in which the adsorbate molecules are distributed on all adsorbent surfaces (Langmuir, 1918). This monolayer adsorption process is also confirmed by the Jovanovic model, which describes monolayer adsorption without the presence of lateral interactions (Ayawei *et al.*, 2017). In the Langmuir model, adsorption is advantageous

or not explained by the R_L value, where the resulting R_L value is between 0 and 1, which indicates the adsorption process is favorable. Meanwhile, Freundlich, Temkin, Dubinin-Radushkevich, and Halsey isotherms support multilayer adsorption processes. The degree of linearization between adsorbate and adsorbent is indicated by the values of $n < 1$ and $1/n > 1$ in the Freundlich model, the values show that adsorption follows cooperative adsorption with chemical interactions. Cooperative adsorption informs the occurrence of chemical and physical interactions at one time (Liu, 2015). The chemical interaction in the adsorption system is in accordance with the parameter value $B_T > 8$ J/mol in the Temkin model. The Dubinin-Radushkevich model also confirmed the physical interaction because the parameter value $E < 8$ kJ/mol.

5.1. Prediction Model for CPS Adsorbent

The adsorption system uses CPS adsorbent following the Langmuir and Jovanovic model which assumes monolayer adsorption. The CPS adsorption system is also compatible with the Harkin-Jura model which assumes multilayer adsorption. Adsorption system using CPS shows weak physical interaction (adsorbent-adsorbate interaction) and chemical interaction (adsorbate-adsorbate interaction). Prediction model for CPS adsorbent is illustrated in **Figure 12**.

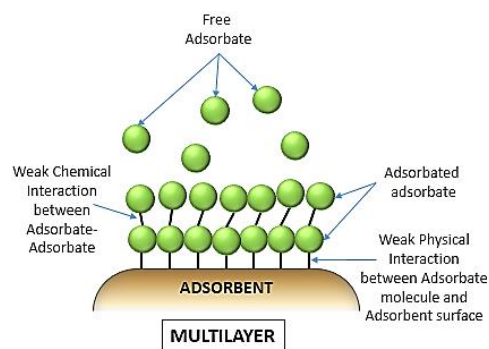


Figure 12. Prediction model for system adsorption using CPS adsorbent

5.2. Prediction Model for CRH Adsorbent

The adsorption system uses CRH adsorbent following the Langmuir and Jovanovic model which assumes monolayer adsorption with weak interaction between adsorbate-adsorbent (physical interaction) since the K_L has small values based on Langmuir. Prediction model for CPS adsorbent is illustrated in **Figure 13**.

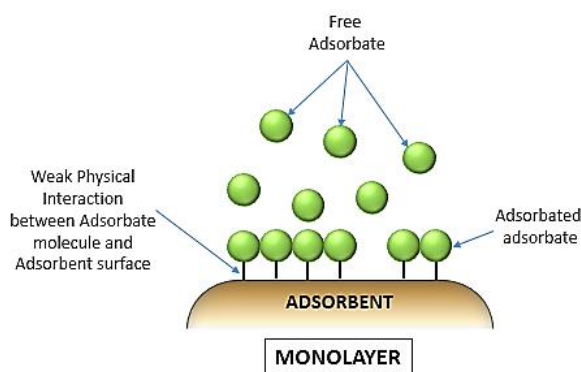


Figure 13. Prediction model for system adsorption using CRH adsorbent

5.3. Prediction Model for SRH and WO_3 Adsorbents

The adsorption system uses SRH and WO_3 adsorbents following monolayer and multilayer adsorption with weak chemical interaction (adsorbate-adsorbate interaction) and physical interaction (adsorbate-adsorbent interaction) since the K_L and A_T have small values based on Langmuir and Temkin parameter respectively. The multilayer adsorption process results from the presence of a heterogeneous structure in the adsorbent which is assumed by the Temkin, Dubinin-Radushkevich, Harkin-Jura, and Halsey isotherm where filling pores occur (Dada et al., 2012). Prediction model for CPS adsorbent is illustrated in **Figure 14**.

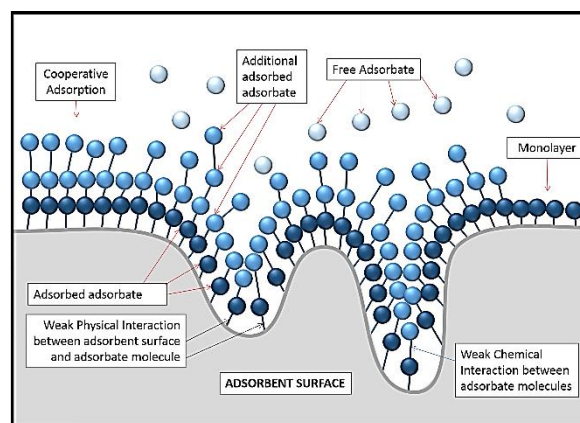


Figure 14. Prediction model for system adsorption using SRH and WO_3 adsorbents

5. CONCLUSION

This study demonstrates a simple way of understanding the calculation of the results of the adsorption data analysis by matching and reviewing the adsorption data in several adsorption isotherm models and demonstrating its application for the adsorption system of various adsorbents. The criteria for selecting a suitable and optimal adsorption isotherm model for the adsorption process have also been discussed in this study. Based on our study, the adsorption system with carbon obtained from peanut shells and carbon obtained from rice husks followed the Jovanovic isotherm. Adsorption system with silica adsorbent extracted from rice husk and WO_3 following Langmuir, Freundlich, Temkin, Dubinin-Radushkevich, Halsey, Jovanovic isotherms.

6. AUTHORS' NOTE

The authors declare that there is no conflict of interest regarding the publication of this article. Authors confirmed that the paper was free of plagiarism.

7. REFERENCES

Afonso, R., Gales, L., and Mendes, A. (2016). Kinetic derivation of common isotherm equations

- for surface and micropore adsorption. *Adsorption*, 22(7), 963-971.
- Afroze, S., and Sen, T. K. (2018). A review on heavy metal ions and dye adsorption from water by agricultural solid waste adsorbents. *Water, Air, & Soil Pollution*, 229(7), 1-50.
- Al-Ghouti, M. A., and Da'ana, D. A. (2020). Guidelines for the use and interpretation of adsorption isotherm models: A review. *Journal of Hazardous Materials*, 393, 122383.
- Anshar, A. M., Taba, P., and Raya, I. (2016). Kinetic and Thermodynamics Studies the Adsorption of Phenol on Activated Carbon from Rice Husk Activated by ZnCl₂. *Indonesian Journal of Science and Technology*, 1(1), 47-60.
- Ayawei, N., Ebelegi, A. N., and Wankasi, D. (2017). Modelling and interpretation of adsorption isotherms. *Journal of chemistry*, 2017.
- Barakat, M. A. (2011). New trends in removing heavy metals from industrial wastewater. *Arabian journal of Chemistry*, 4(4), 361-377.
- Crini, G., and Badot, P. M. (2008). Application of chitosan, a natural aminopolysaccharide, for dye removal from aqueous solutions by adsorption processes using batch studies: a review of recent literature. *Progress in Polymer Science*, 33(4), 399-447.
- Dąbrowski, A. (2001). Adsorption—from theory to practice. *Advances in Colloid and Interface Science*, 93(1-3), 135-224.
- Dada, A. O., Olalekan, A. P., Olatunya, A. M., and Dada, O. J. I. J. C. (2012). Langmuir, Freundlich, Temkin and Dubinin–Radushkevich isotherms studies of equilibrium sorption of Zn²⁺ onto phosphoric acid modified rice husk. *IOSR Journal of Applied Chemistry*, 3(1), 38-45.
- Fiandini, M., Ragadhita, R., Nandiyanto, A. B. D., and Nugraha, W. C. (2020). Adsorption characteristics of submicron porous carbon particles prepared from rice husk. *J. Eng. Sci. Technol*, 15, 022-031.
- Foo, K. Y., and Hameed, B. H. (2009). Utilization of biodiesel waste as a renewable resource for activated carbon: application to environmental problems. *Renewable and Sustainable Energy Reviews*, 13(9), 2495-2504.
- Ghani, S. A. A. (2015). Trace metals in seawater, sediments and some fish species from Marsa Matrouh Beaches in north-western Mediterranean coast, Egypt. *The Egyptian Journal of Aquatic Research*, 41(2), 145-154.
- Guddati, S., Kiran, A. S. K., Leavy, M., and Ramakrishna, S. (2019). Recent advancements in additive manufacturing technologies for porous material applications. *The International Journal of Advanced Manufacturing Technology*, 105(1), 193-215.
- Gupta, V. K. (2009). Application of low-cost adsorbents for dye removal—a review. *Journal of Environmental Management*, 90(8), 2313-2342.
- Hegazi, H. A. (2013). Removal of heavy metals from wastewater using agricultural and industrial wastes as adsorbents. *HBRC Journal*, 9(3), 276-282.
- Hamdaoui, O., and Naffrechoux, E. (2007). Modeling of adsorption isotherms of phenol and chlorophenols onto granular activated carbon: Part I. Two-parameter models and

- equations allowing determination of thermodynamic parameters. *Journal of Hazardous Materials*, 147(1-2), 381-394.
- Holkar, C. R., Jadhav, A. J., Pinjari, D. V., Mahamuni, N. M., and Pandit, A. B. (2016). A critical review on textile wastewater treatments: possible approaches. *Journal of Environmental Management*, 182, 351-366.
- Kadja, G., and Ilmi, M. M. (2019). Indonesia natural mineral for heavy metal adsorption: A review. *Journal of Environmental Science and Sustainable Development*, 2(2), 3.
- Kong, L., and Adidharma, H. (2019). A new adsorption model based on generalized van der Waals partition function for the description of all types of adsorption isotherms. *Chemical Engineering Journal*, 375, 122112.
- Langmuir, I. (1918). The adsorption of gases on plane surfaces of glass, mica and platinum. *Journal of the American Chemical Society*, 40(9), 1361-1403.
- Liu, S. (2015). Cooperative adsorption on solid surfaces. *Journal of Colloid and Interface Science*, 450, 224-238.
- Maryanti, R., Nandiyanto, A. B. D., Manullang, T. I. B., & Hufad, A. (2020). Adsorption of Dye on Carbon Microparticles: Physicochemical Properties during Adsorption, Adsorption Isotherm and Education for Students with Special Needs. *Sains Malaysiana*, 49(12), 2949-2960.
- Naggar, Y. A., Naiem, E., Mona, M., Giesy, J. P., and Seif, A. (2014). Metals in agricultural soils and plants in Egypt. *Toxicological & Environmental Chemistry*, 96(5), 730-742.
- Nandiyanto, A. B. D., Girsang, G. C. S., Maryanti, R., Ragadhita, R., Anggraeni, S., Fauzi, F. M., and Al-Obaidi, A. S. M. (2020a). Isotherm adsorption characteristics of carbon microparticles prepared from pineapple peel waste. *Communications in Science and Technology*, 5(1), 31-39.
- Nandiyanto, A. B. D. (2020b). Isotherm adsorption of carbon microparticles prepared from pumpkin (*Cucurbita maxima*) seeds using two-parameter monolayer adsorption models and equations. *Moroccan Journal of Chemistry*, 8(3), 8-3.
- Ragadhita, R., Nandiyanto, A. B. D., Nugraha, W. C., and Mudzakir, A. (2019). Adsorption isotherm of mesopore-free submicron silica particles from rice husk. *Journal of Engineering Science and Technology*, 14(4), 2052-2062.
- Nandiyanto, A. B. D., Arinalhaq, Z. F., Rahmadiani, S., Dewi, M. W., Rizky, Y. P. C., Maulidina, A., and Yunas, J. (2020c). Curcumin Adsorption on Carbon Microparticles: Synthesis from Soursop (*Annona Muricata* L.) Peel Waste, Adsorption Isotherms and Thermodynamic and Adsorption Mechanism. *International Journal of Nanoelectronics and Materials*, 13 (Special Issue Dec 2020), 173-192
- Nandiyanto, A. B. D., Maryanti, R., Fiandini, M., Ragadhita, R., Usdiyana, D., Anggraeni, S., and Al-Obaidi, A. S. M. (2020d). Synthesis of Carbon Microparticles from Red Dragon Fruit (*Hylocereus undatus*) Peel Waste and Their Adsorption Isotherm Characteristics. *Molekul*, 15(3), 199-209.
- Nandiyanto, A. B. D., Ragadhita, R., & Yunas, J. (2020e). Adsorption Isotherm of Densed

Monoclinic Tungsten Trioxide Nanoparticles. *Sains Malaysiana*, 49(12), 2881-2890.

- Nandiyanto, A. B. D., Erlangga, T. M. S., Mufidah, G., Anggraeni, S., Roil, B., & Jumril, Y. (2020f). Adsorption isotherm characteristics of calcium carbonate microparticles obtained from barred fish (*Scomberomorus* spp.) bone using two-parameter multilayer adsorption models. *International Journal of Nanoelectronics and Materials*, 13 (Special Issue Dec 2020), 45-58.
- Nandiyanto, A. B. D., Ragadhita, R., Oktiani, R., Sukmafitri, A., and Fiandini, M. (2020g). Crystallite sizes on the photocatalytic performance of submicron WO_3 particles. *Journal of Engineering Science and Technology*, 15(3), 1506-1519.
- Rahmani, M., and Sasani, M. (2016). Evaluation of 3A zeolite as an adsorbent for the decolorization of rhodamine B dye in contaminated waters. *Applied Chemistry*, 11(41), 83-90.
- Romero-Gonzalez, J., Peralta-Videa, J. R., Rodriguez, E., Ramirez, S. L., and Gardea-Torresdey, J. L. (2005). Determination of thermodynamic parameters of Cr (VI) adsorption from aqueous solution onto *Agave lechuguilla* biomass. *The Journal of Chemical Thermodynamics*, 37(4), 343-347.
- Saadi, R., Saadi, Z., Fazaeli, R., and Fard, N. E. (2015). Monolayer and multilayer adsorption isotherm models for sorption from aqueous media. *Korean Journal of Chemical Engineering*, 32(5), 787-799.
- Sert, E. B., Turkmen, M., and Cetin, M. (2019). Heavy metal accumulation in rosemary leaves and stems exposed to traffic-related pollution near Adana-Iskenderun Highway (Hatay, Turkey). *Environmental Monitoring and Assessment*, 191(9), 1-12.
- Shanavas, S., Kunju, A. S., Varghese, H. T., and Panicker, C. Y. (2011). Comparison of Langmuir and Harkins-Jura adsorption isotherms for the determination of surface area of solids. *Oriental Journal of Chemistry*, 27(1), 245.